

JULY 25 2023

# Temperature-induced sound speed variability in a laboratory water tank **FREE**

Alexandra M. Hopps-McDaniel; Tracianne B. Neilsen 



*Proc. Mtgs. Acoust* 51, 070001 (2023)

<https://doi.org/10.1121/2.0001757>



View  
Online



Export  
Citation

CrossMark



 **ASA**

Advance your science and career as a member of the  
**Acoustical Society of America**

[LEARN MORE](#)



## 184th Meeting of the Acoustical Society of America

Chicago, Illinois

8-12 May 2023

### Underwater Acoustics: Paper 3pUW2

# Temperature-induced sound speed variability in a laboratory water tank

**Alexandra M. Hopps-McDaniel and Tracianne B. Neilsen**

*Department of Physics and Astronomy, Brigham Young University, Provo, UT, 84602;  
mcdaniel.alexh@gmail.com; tbn@byu.edu*

Temperature variations in the ocean cause changes in the sound speed and, hence, sound propagation. This project quantified the sound speed variation achievable in a laboratory water tank. The rectangular tank has paneling that minimizes lateral reflections. Two temperature sensors measured the temperature changes over time while the water was cooled with ice, heated, and naturally warmed back to room temperature. Sound speed values were calculated using the freshwater Marczak equation. We found that while the temperature remains relatively uniform near the bottom of the tank during heating and cooling. Heating increases the sound speed at a rate of 3.5 m/s per hour, while adding ice in various quantities decreases the temperature rapidly. After rapid cooling, the water near the surface of the tank warms faster than the water near the bottom, creating a depth-dependent sound speed gradient. Eight hours after adding 380 pounds of pebble ice, the sound speed gradient was 10.7 m/s per meter. The water temperature variability in these tank measurements replicates a portion of the sound speed variability seen in the ocean. This sound speed variability can then be used to test the robustness of machine learning algorithms.



## 1. INTRODUCTION

With new advances in machine learning (ML), large data sets can be processed to discover new features and accomplish tasks such as target classification and source localization. ML, which is entirely data-driven, has the potential to identify acoustics features by learning to identify patterns in data. ML has a lot of potential for accurate and real-time acoustics predictions.<sup>1</sup> Potential applications in ocean acoustics are, however, complicated by the spatial and temporal variability in the ocean environment.

Traditionally, sound propagation in the ocean has been modeled numerically, and optimizations have been used to estimate properties, such as source location. For example, matched-field processing (MFP) has often been used to locate sources in range, depth, and azimuth. The accuracy of MFP depends on how the ocean environment is represented in the sound propagation model.<sup>2,3</sup> MFP source localization was compared to ML source localization in several studies. For example, Lefort *et al.*<sup>4</sup> compared ML source localization to MFP using laboratory tank data. Comparisons with ocean data have also been performed, such as the study by Niu *et al.*<sup>5</sup> They used data collected by a vertical line array (VLA) in the Santa Barbara Channel of three ship tracks. The data while ships traveled along one track were used for training purposes, and data samples from two other ship tracks were used for testing. They showed that ML outperforms MFP for longer ranges when limited environmental knowledge is known. Specifically, MFP techniques localized the ships accurately up to 4 km away, however, after 4 km, MFP lost accuracy. The ML predicted location of the two ships, however, remained accurate for the entire 9 km range, as shown in their Fig. 3.

From this study and others, we anticipate benefits from using ML because it does not require sound propagation modeling. Instead, the variability due to environmental parameters is incorporated during training.<sup>4,5</sup> A study done by Van Komen *et al.*<sup>6</sup> shows the importance of accounting for ocean variability during the training step of machine learning. The conclusion was that training with greater sound speed variability leads to better generalization. Their work is one example of how the robustness of machine learning algorithms needs to be tested against a variety of environmental complexities.<sup>7</sup>

For investigations into building ML applications that are robust in light of environmental uncertainty, we plan to use acoustic data measured in a laboratory water tank with variable conditions. In preparation for this work, the amount of sound speed variability currently achievable in the tank is investigated. The goal of this paper is to demonstrate the range of temporal and spatial sound speed variability possible in our laboratory tank due to an advanced heating/filtration system and the addition of ice. A description of the experimental setup and the results of several experiments are presented.

## 2. BACKGROUND

In this section, background is provided about sound speed variability in the ocean. Previous work by others on establishing sound speed variability in laboratory tanks is then discussed.

### A. SOUND SPEED VARIABILITY

Many physical phenomena contribute to the temporal and spatial variations in sound speed in shallow oceans. These variations depend on weather, seasons, and latitude and are influenced by

internal gravity waves. Rossing<sup>8</sup> discusses some of the seasonal effects on sound speed profiles in the *Springer Handbook of Acoustics*. Winter months typically show an isovelocity effect due to mixing, which produces sound speed profiles that are relatively constant with depth. In summer months, however, water is typically warmer near the surface from solar heating. In that text, examples in Fig. 5.4 on p. 152 show general sound speed profiles in winter versus summer months. In winter months, the sound velocity stays close to 1500 m/s from the surface to a depth of 100 m. For summer months, however, the upper 20 m is well mixed at around 1530 m/s, from 20 m to 40 m the sound speed drops rapidly to 1500 m/s, and below that stays fairly constant to the seafloor.<sup>8</sup>

Differences in sound speeds change the acoustic propagation paths. An experiment published by Sertlek *et al.*<sup>9</sup> examines how assuming a constant sound speed in the water column rather than a sound speed gradient affects the accuracy of shipping sound maps. The study was done on data measured in the Dutch North Sea (water depth of 70 m), where sound speed in the summer months can vary as a function of depth from 1480 m/s to 1515 m/s while varying in winter between 1465 m/s and 1480 m/s. (See Fig. 2 from that paper.) They compared sound pressure level (SPL) during the winter and summer measurements to the SPL assuming an isovelocity sound speed profile. Relative to the isovelocity case, the winter measurements differed by 2.5 dB and the summer measurements by 5 dB over a wide frequency band.

In addition to seasonal changes, spatial variations in sound speed profiles also occur. During the Seabed Characterization Experiment (2022), sound speed profiles (SSP) from the New England Mud patch were taken at various locations. Two measured SSPs are shown in Fig. 1. In the northern regions of the New England Mud patch (a), the sound speed stayed nearly uniform from the middle of the water column to the ocean floor. However, the SSP at the southern location (b) showed a rapid increase in sound speed near the ocean floor due to warmer water brought up by currents from the south. The distance between the two SSPs was 5.56 km. Spatial variations in the SSP in the New England Mud Patch add a layer of complication to the analysis of data collected during the experiment.

The last cause of sound speed variation in the ocean discussed here is internal gravity waves, which are found in greater quantities near the coast. These waves introduce more scattering and a time-dependent complexity that is difficult to model.<sup>7</sup> Badiy *et al.*<sup>10</sup> analyzed data from the Shallow Water Acoustic Experiment 2006 (SW06) conducted on the New Jersey continental shelf to record the time-varying environment induced by nonlinear internal waves (NLIWs). Figure 3d of their publication shows time-varying temperature fluctuations over a span of 5 hours. At times, the water temperature at the specified location is isothermal, however, at other times large spikes in the water temperature cause up to a 15°C increases. The temperature fluctuations vary in depth, repetition rate, and have duration of up to 10 minutes. Their Fig. 1e also shows the range-dependent temperature fluctuations of about 20°C over a 3 km change in distance from the shore.

## B. WATER TANKS

Many labs choose to use a laboratory water tank for collecting scale-model acoustics data. Sagers and Ballard<sup>11</sup> discuss the use of scale-model laboratory experiments as useful for the development of three-dimensional acoustic propagation models. They assert that laboratory tanks can be used to collect benchmark data, as data measured in the ocean has insufficient environmental information for modeling, along with time-dependent variations in the ocean environment.

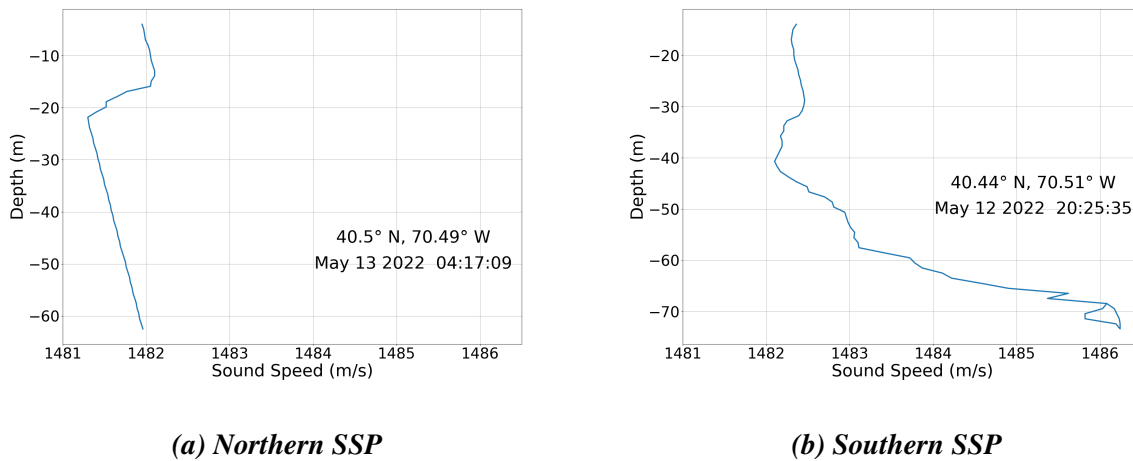


**Figure 1:** Two sound speed profiles taken in the New England Mud Patch in May. The southern SSP cast was taken 5.56 km south of the northern cast. The southern cast shows the effect of warmer water currents increasing the temperature of the water near the bottom.

In contrast, water tank measurements allow for greater control and knowledge of environmental information that provides more consistent modeling. In a water tank, temperature, bathymetry, altimetry, source/receiver geometry, bottom roughness, etc. can all be maintained. Additionally, complications resulting from additional sounds from shipping lanes and other ambient noises in the ocean are eliminated.

Though laboratory tanks are used to create a controlled environment for testing acoustics models, complications arise in making the tank into a scale model of the ocean. Some of these complications arise due to lateral reflections and determining properties of the materials used for the bottom of the laboratory tank. Attempts to scale frequency and distances are complicated by the fact that attenuation is not a linear function of frequency. Finally, a room-temperature water tank defaults to uniform sound speed, where SSPs vary widely in the ocean, as detailed above.

Attempts to mitigate this sound speed limitation have been undertaken by two labs that successfully varied the sound speed gradient in a laboratory water tank. Zhang and Swinney<sup>12</sup> created a sound speed gradient in their tank by linearly increasing the salinity (density) of the water in their 0.9 m long and 0.45 m wide tank at a depth of 0.5 m. The density and thereby sound speed varied continuously, achieving speeds of 1500 to 1700 m/s and a depth-dependant sound speed gradient of 0.377 m/s per mm.

In another paper, Rabau<sup>13</sup> discussed their different approach of using liquids of different densities to create the sound speed gradient. The dimensions of the tank were 4.5 m long and 0.88 m wide. The fluids used included two aqueous alcohol mixtures and four saline solutions and totaled a depth of 20 cm. The sound speed profile the laboratory replicated was that of a tropical eastern summer in the deep ocean (4 km depth). They were able to create a laboratory sound speed profile with an axis of minimum sound speed or a SOFAR channel. The sound speeds ranged from 1490 to 1520 m/s. Furthermore, the layered liquids were able to maintain their separation for several hours. Their Fig. 8 shows the sound speed profile evolution over one week.

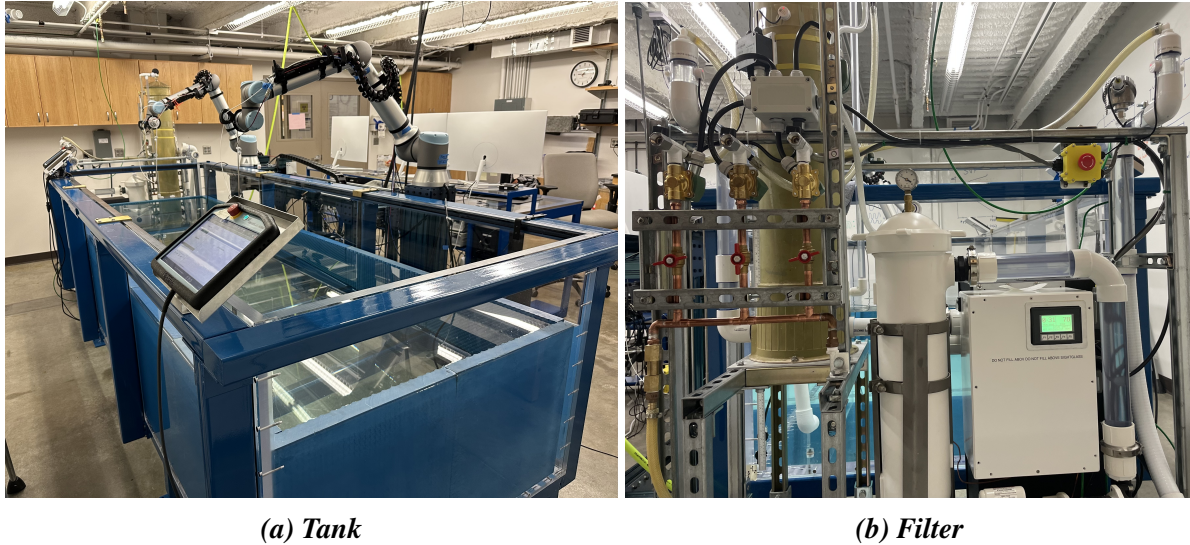


**Figure 2:** (a) Laboratory set-up. (b) Advanced filtration system with heater and debubbler tower that can heat water ranging from 19°C to 38°C.

Another group conducted experiments in a laboratory tank with an acoustic lens to simulate the refraction caused by the passage of internal waves.<sup>14</sup> Their tank was 3 m long, 1 m wide, and 1 m deep. The acoustic lens had a square cross-section of 0.15 m x 0.15 m and the water was 0.02 m deep. High-frequency ultrasound (2.25 MHz) traveled through a Plexiglas plano-concave lens. The resulting sound field contained shadow zones and caustics, as are often found in the ocean, especially during the passage of internal waves.<sup>15</sup>

Tank data have also previously been used in machine-learning applications.<sup>4,16</sup> Because machine learning is dependent on having a large source of data, water tanks make an ideal place for training and testing machine-learning models. Yangzhou *et al.*<sup>16</sup> conducted an experiment to test a deep neural network (DNN) approach to source localization and compared results to several MFP approaches. For their experiment, they used uncalibrated hydrophones to demonstrate the robustness of a DNN method in a 1.1 m x 1.4 m tank with a water depth of 10 mm. For each frequency, they gathered 8000 samples of data and used 7200 for training purposes and the rest for testing. Their Table II shows that a DNN method far surpasses MFP in accuracy. The primary conclusion of their work is that DNN method is advantageous because it does not rely on an acoustic forward model or sensor calibration.

With all of this in mind, the goal of the experiment reported here is to use temperature to vary the sound speed of a laboratory water tank for testing the robustness of machine learning algorithms. Other labs have either created variable sound speeds in water tanks or have performed machine-learning experiments with tank data. Our lab hopes to combine the two by introducing sound speed variability into a machine-learning experiment.

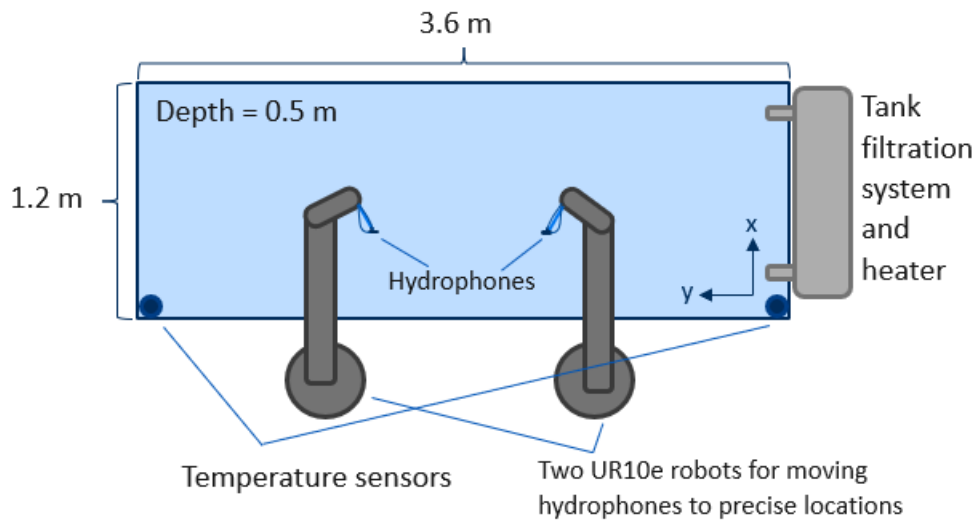


*Figure 3: Diagram of water tank and automatic positioning system.*

### 3. METHODS

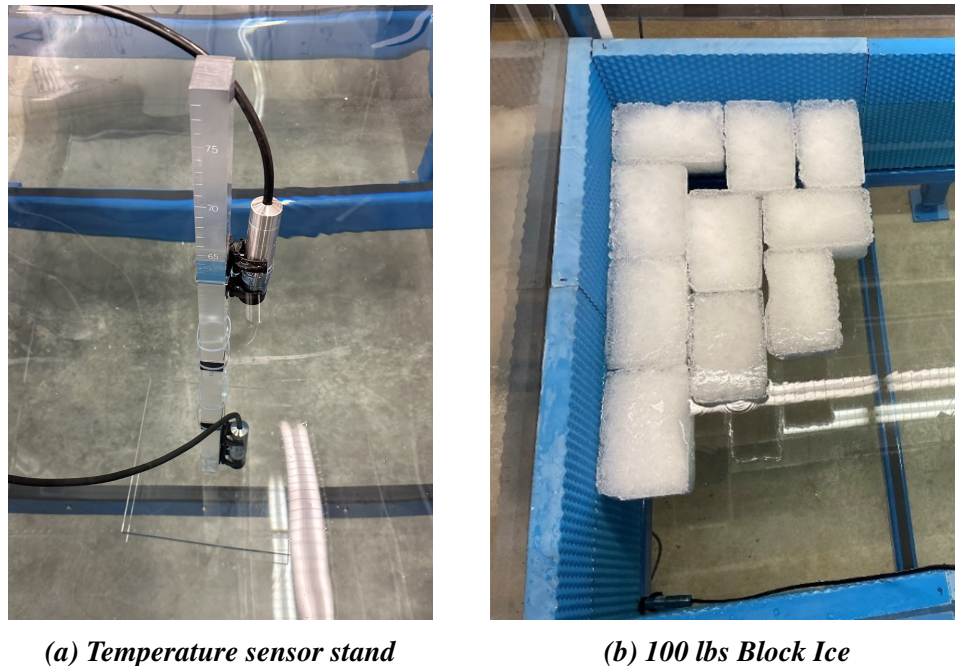
#### A. MEASUREMENT SETUP

The water tank in this experiment, shown in Fig. 2(a), has dimensions of 1.2 m x 3.6 m and holds a maximum depth of 0.91 m, which equates to a max water volume of 4077.6 L. The tank is made of acrylic because its acoustic impedance is more similar to water than tanks made from steel, concrete, or glass. The material has added benefits of being transparent and non-corrosive. To further minimize reflections from the sides of the tank, panels made of polyurethane are placed in the tank. This attenuating material from Precision Acoustics Ltd. advertises echo reduction greater than 30 dB for frequencies in the 20-200 kHz range.

On one side of the tank is a water filter and heater, as shown in Fig. 2(b). The water filter was designed to keep the water well sanitized and has a custom-made debubbler tower.<sup>17</sup> Additionally, chemicals are added to the tank weekly to ensure consistent conditions of the water. Tap water is used to fill the tank as it is less corrosive to the acrylic than distilled. Distilled water is used to replace evaporated water to maintain consistent mineral content. The heater attached to the water filter can output water ranging from 19°C to 38 °C.

Alongside the water tank are two UR10e robots from Universal-Robots. The robots are used as a positioning system as they each have six axes of motion and a reach of 1.3 m. One of the robots is mounted on an extender track, giving it 1.4 m added reach. This underwater positioning system has an uncertainty of  $\pm 0.01$  mm for repeat measurement. The robots move transmitters, receivers, and temperature sensors to precise locations in the tank. A diagram of the water tank is included in Fig. 3.

The positions and data acquisition are controlled via a custom LabVIEW software called Easy Spectrum Acoustics Underwater (ESAU) because it uses spectrum 16-bit data acquisition cards. This software was edited to include a temperature recording capability for a selected number of



(a) Temperature sensor stand

(b) 100 lbs Block Ice

**Figure 4:** (a) Two temperature probes attached to a stand designed to place the probes at specified depths within the water tank. (b) Beginning of Experiment B when 100 lbs of block ice was added to the tank.

hours. More information on the design of the laboratory water tank and the data acquisition system used in this experiment can be found in the Vongsawad *et al.*<sup>17</sup>

## B. TEMPERATURE EXPERIMENTS

At room temperature, a water tank tends to have a spatially uniform water temperature producing constant sound speed throughout the water. Experiments were performed to test the sound speed variation attainable in our water tank using heating and adding ice. From these experiments, we can assess the minimum and maximum sound speed caused by ice and the tank heater and establish if a depth-dependent sound speed gradient occurs during the various stages of warming and cooling.

Temperature measurements are made with two LMP 307T depth and temperature transmitters, which specify an accuracy of less than or equal to 1 degree Celsius. During a calibration test of the two sensors in a bath of ice water, the temperature sensors measured about 0.05°C different. This difference in calibration corresponds to a difference of sound speed of less than 0.15 m/s for water at 20°C. During the experiments, the temperature is sampled every 5 sec and saved to Excel spreadsheets. These data are then plotted and converted to water sound speed with Python.

The time-dependent water temperatures were used in the Marczak<sup>18</sup> empirical equation for obtaining fresh water sound speed as a function of temperature only. The equation is a fifth-order polynomial that is valid from 0 to 95°C and is shown in their Eq. (1) and Table 2.

The locations of the temperature sensors for the four experiments are listed in Table 1. The  $(x, y, z)$  coordinates of the temperature sensors are measured from the axis at the bottom right



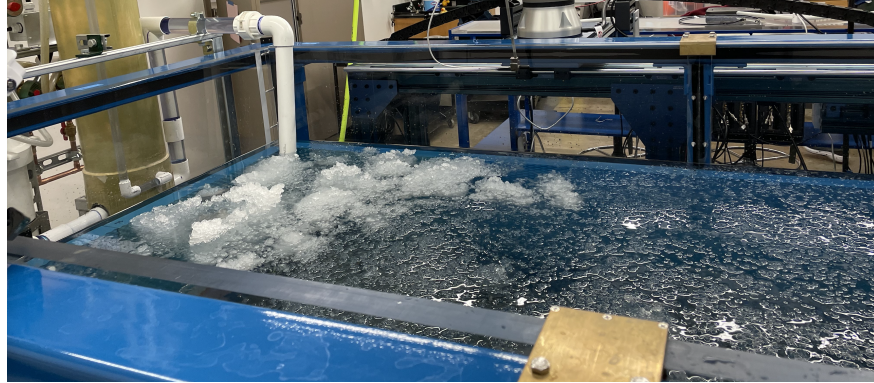


**Figure 5: Beginning of Experiment C with 300 lbs of pebble ice in tank.**

corner of the tank, as illustrated in Fig. 3.

Experiments A and B were the first two time-dependent measurements taken. The temperature sensors were at the same depth in the water tank for the entirety of data collection. For Experiment A, the temperature sensors were at opposite ends of the tank located at the bottom and the initial water depth was 0.5 m. The tank was heated for two hours with the filter temperature set at 38°C, with Sensor 2 located closer to the outlet of the water heater. For Experiment B, the temperature sensors were once again placed on opposite ends of the water tank near the bottom. The initial water depth was 0.43 m for this experiment and 100 pounds of block ice were added. (See Fig. 3b.)

Experiments C and D were both time and depth-dependent, meaning the temperature sensors were placed at the center of the tank at different depths as seen in Fig. 4(a). For Experiment C, the initial water depth was 0.6 m. Sensor 1 was 5 cm, below the water line and Sensor 2 was located 1 cm, from the bottom of the tank. During this experiment, the heater ran for two hours set at 38°C. Approximately 20 minutes after the heater was turned on, 300 lbs of pebble ice were added. (See Fig. 5.) For Experiment D, 380 lbs of pebble ice were added and the heater was not on during the experiment. The initial water depth was 0.5 m and Sensor 1 was 7 cm, below the water line and Sensor 2 was located 1 cm, above the bottom of the tank.

The hypothesis was that ice added in hundreds of pounds to the surface of the tank decreases the sound speed near the surface, and the heater which better mixes water at the bottom of the tank increases sound speed faster lower in the water. This effect would ideally cause SSPs in our tank similar to profiles found where warm water currents traveling along the bottom of the ocean floor increase the sound speed at deeper depths, similar to the southern profile from the New England Mud Patch. (See Fig. 1.)

## 4. RESULTS

The results from all four experiments are presented. In all plots in this section, the blue line represents Sensor 1 and the orange line is Sensor 2. The legend of the plots gives information on the depth of the sensors, not the z-coordinates. (See Table 1 for details of the experiments.)

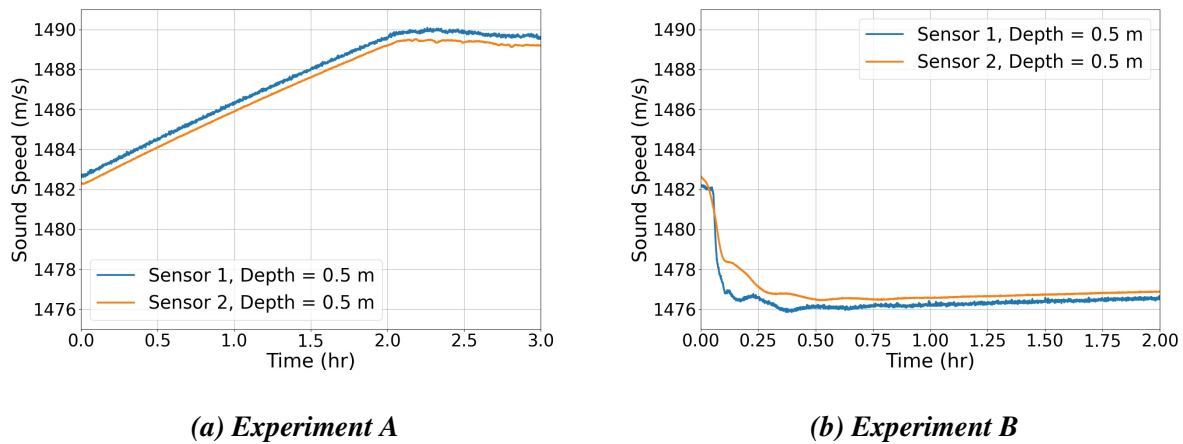


**Figure 6:** (a) Sound speed at the bottom of the tank was measured with two temperature sensors. The water was heated at  $38^{\circ}\text{C}$  for 2 hours and cooling was tracked for an hour after. (b) Sound speed at the bottom of the tank after 100 lbs of block ice were added to the tank. Two hours of data are shown.

**Table 1: Temperature Experiments.**

Experiment	Method	Water Depth	Locations	
			Sensor 1	Sensor 2
A	2 hr heating	0.5 m	(0,L,0)	(0,0,0)
B	100 lbs block ice	0.43 m	(0,L,0)	(0,0,0)
C	300 lbs pebble ice and heat	0.6 m	(0.6,1.8,0.55)	(0.6,1.8,0.01)
D	380 lbs pebble ice	0.5 m	(0.6,1.8,0.43)	(0.6,1.8,0.01)

## A. TIME-DEPENDENCE

The sound speed for the experiments A and B are shown in Fig. 6. The plot (a) shows that the two hours of heating in Experiment A resulted in a 7 m/s increase in sound speed. As the water was heated, the sound speed increased linearly at a rate of 3.5 m/s per hour. Comparing the temperature from Sensors 1 and 2, the sound speed in the tanks maintained a difference of approximately 0.3 m/s throughout the experiment. This relates to a temperature difference of less than 0.2 degrees Celsius, which is similar to the difference in calibration. Though farther from the water heater, Sensor 1 and Sensor 2 measured approximately the same temperatures as soon as data acquisition began even with the water heater being closer to one probe. One explanation is that the water is well enough mixed, due to the flow caused by the filter, to maintain uniform sound speed across the bottom of the tank. Additional trials have proved that additional hours of heating can extend the sound speeds at the same linear rate.

The plot for Experiment B (Fig. 6(b)) shows that adding block ice rapidly decreased the sound

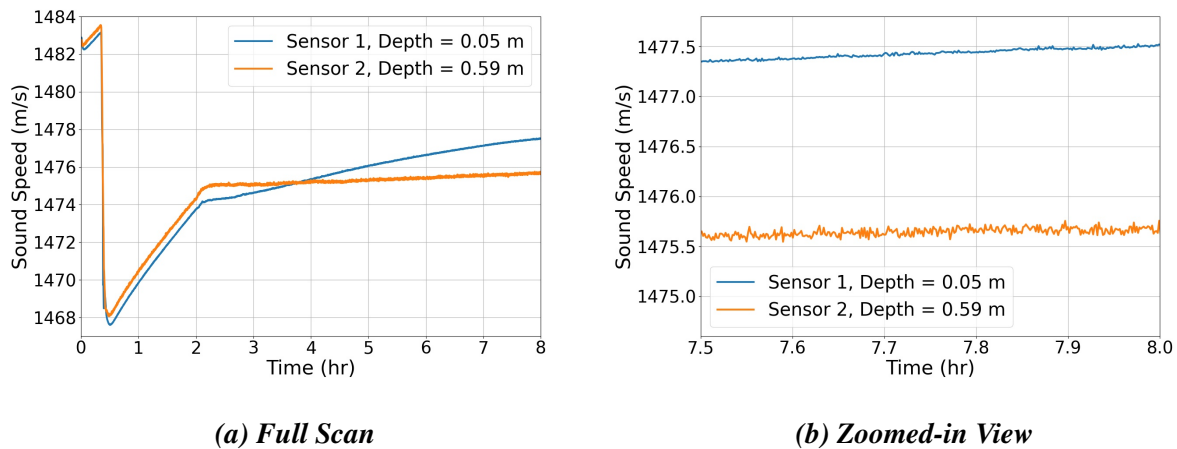


**Figure 7: Sound speeds during Experiment C with 300 lbs of pebble ice and two hours of heating at 38°C.**

speed in the water tank. One-hundred pounds of ice blocks decreased the temperature of the water at the bottom of the tank by 6 m/s. Sensor 1 was located closer to the block ice when they were added to the tank, which explains why the temperature near Sensor 1 dropped faster than Sensor 2. However, even with the water heater turned off, enough mixing occurred in the tank that the temperature at the bottom of the water tank reached uniformity as shown by both sensors maintaining even spacing beginning at 0.75 hours.

## B. DEPTH-DEPENDENT

The variation in sound speed for the depth-dependent Experiment C is shown in Fig. 7. The full scan plot (a) shows that adding the pebble ice rapidly dropped the sound speed by 15 m/s. This decrease in temperature is constant from the surface to the bottom of the tank even while the heater is running. Again, the heater increases the water temperature linearly. Additionally, these data show that this temperature increase is relatively uniform from surface to bottom. Once the heater is turned off, the water continues to warm back up to room temperature, and only then does the water temperature show a temperature gradient. The temperature near the surface of the water increased faster than the water near the bottom, and the zoomed-in plot (b) shows that over the 0.54 m change in depth, a  $1.8 \pm 0.15$  m/s change in sound speed is established, yielding a sound speed gradient of  $3.3 \pm 0.28$  m/s per m.

Experiment D was a test to see if adding ice without heating would allow for the temperature gradient from surface to bottom to be extended. Figure 8 shows that adding 380 lbs of ice rapidly decreased the temperature of the water between 21 and 22 m/s. From there, the water near the surface warmed faster. The zoomed-in plot (b) between 7.5 and 8 hours after dumping the ice shows about a  $4.5 \pm 0.15$  m/s change in sound speed for a 0.42 m change in depth, yielding a sound speed gradient of  $10.71 \pm 0.35$  m/s per m.

A summary of the results of the temperature experiments is located in Table 2. Experiments A and B do not have values for the depth-dependent sound speed gradient because the sensors were

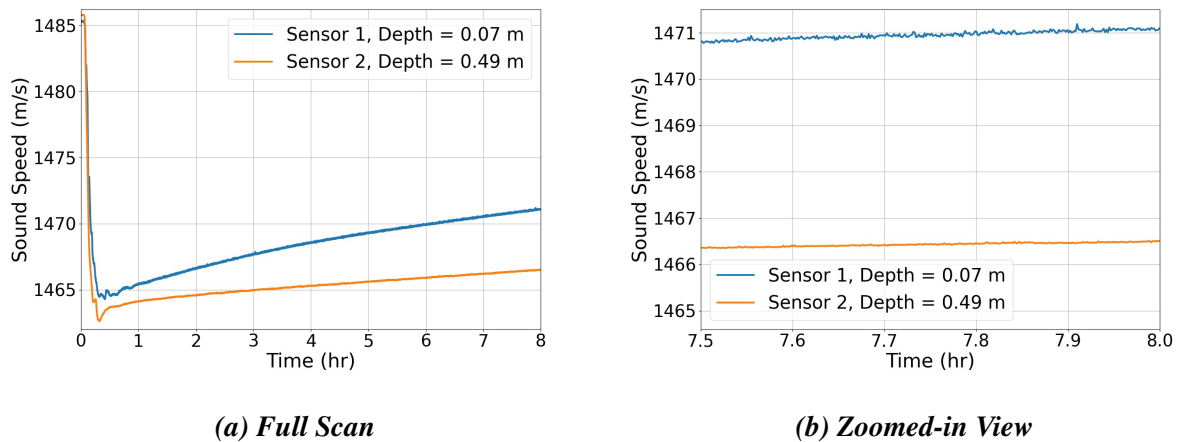


**Figure 8: Sound speeds during Experiment D with 380 lbs of pebble ice added at the beginning.**

**Table 2: Sound Speed (SS) Results.**

Experiment	Max SS	Min SS	Max SS change	SS gradient at 8 hr
A	1490 m/s	1483 m/s	7 m/s	
B	1482 m/s	1476 m/s	6 m/s	
C	1483 m/s	1468 m/s	15 m/s	$3.33 \pm 0.28 \text{ s}^{-1}$
D	1485 m/s	1463 m/s	22 m/s	$10.71 \pm 0.35 \text{ s}^{-1}$

at the same depth for the entirety of the experiment.

## 5. CONCLUSION

Based on these four temperature experiments, we conclude that we are able to successfully attain time-dependent and depth-dependent sound speed variations due to temperature changes in the water. For the time-dependent experiments, two hours of heating results in a linear increase in sound speed at a rate of 3.5 m/s per hour. Adding 100 pounds of block ice decreases the bottom water temperature by 6 m/s. The temperature all along the bottom of the tank remains uniform during both heating and ice experiments.

The depth-dependent experiments showed that there is not much variation of temperature from surface to bottom while the heater is turned on or ice is melting due to mixing. The water near the surface, however, does warm faster than the bottom when going back to room temperature. Eight hours after adding 380 pounds of pebble ice, the sound speed gradient was 10.7 m/s per m. The thermal conductivity of acrylic is  $200 \text{ mW}/(\text{m K})^{19}$  which is about four times greater than that of air, which is  $26 \text{ mW}/(\text{m K})^{20}$ . Thus, we can conclude that it is not the material of the acrylic that is causing the bottom water to warm slower. The more rapid warming near the surface is due to

convection within the water and evaporative cooling as the HVAC duct points at the top of the tank.

In conclusion, we characterized the sound speed variability in our tank and obtained a time-dependent sound speed due to the heater and adding ice, as detailed in Table 2. A depth-dependent sound speed gradient occurred during the natural warming back to room temperature. We anticipate that by cooling the water at the bottom of the tank and heating the surface water, the depth-dependent sound speeds could be larger and more stable. The sound speed variability achievable with our experimental setup will allow for testing the robustness of our machine learning algorithms in upcoming work.

## ACKNOWLEDGMENTS

We would like to acknowledge Adam Kingsley and Jay Clift for helping update the LabVIEW software (ESAU) used for the temperature acquisition for these experiments. A. H-M. thanks the College of Physical and Mathematical Sciences at Brigham Young University for undergraduate research assistantship funding. We also acknowledge support from the Office of Naval Research for funding the experimental setup under grant #N00014-19-1-2683.

## REFERENCES

- <sup>1</sup> M. J. Bianco, P. Gerstoft, J. Traer, E. Ozanich, M. A. Roch, S. Gannot, and C.-A. Deledalle, “Machine learning in acoustics: Theory and applications,” *The Journal of the Acoustical Society of America* **146**(5), 3590–3628 (2019).
- <sup>2</sup> A. B. Baggeroer, W. A. Kuperman, and P. N. Mikhalevsky, “An overview of matched field methods in ocean acoustics,” *IEEE Journal of Oceanic Engineering* **18**(4), 401–424 (1993).
- <sup>3</sup> A. B. Baggeroer and W. A. Kuperman, “Matched field processing in ocean acoustics,” *Acoustic signal processing for ocean exploration* 79–80 (1993).
- <sup>4</sup> R. Lefort, G. Real, and A. Drémeau, “Direct regressions for underwater acoustic source localization in fluctuating oceans,” *Applied Acoustics* **116**, 303–310 (2017).
- <sup>5</sup> H. Niu, E. Ozanich, and P. Gerstoft, “Ship localization in santa barbara channel using machine learning classifiers,” *The Journal of the Acoustical Society of America* **142**(5), EL455–EL460 (2017).
- <sup>6</sup> D. F. Van Komen, K. Howarth, T. B. Neilsen, D. P. Knobles, and P. H. Dahl, “A cnn for range and seabed estimation on normalized and extracted time-series impulses,” *IEEE Journal of Oceanic Engineering* **47**(3), 833–846 (2022).
- <sup>7</sup> W. A. Kuperman and J. F. Lynch, “Shallow-water acoustics,” *Physics Today* **57**(10), 55–61 (2004).
- <sup>8</sup> T. D. Rossing, *Springer Handbook of Acoustics* (Springer, 2014), pp. 151–152.

- 
- <sup>9</sup> H. Ö. Sertlek, B. Binnerts, and M. A. Ainslie, “The effect of sound speed profile on shallow water shipping sound maps,” *Journal of the Acoustical Society of America* **140**(1), EL84–EL88 (2016).
- <sup>10</sup> M. Badiy, L. Wan, and J. F. Lynch, “Statistics of nonlinear internal waves during the shallow water 2006 experiment,” *Journal of Atmospheric and Oceanic Technology* **33**(4), 839–846 (2016).
- <sup>11</sup> J. D. Sagers and M. S. Ballard, “Testing and verification of a scale-model acoustic propagation system,” *The Journal of the Acoustical Society of America* **138**(6), 3576–3585 (2015).
- <sup>12</sup> L. Zhang and H. L. Swinney, “Sound propagation in a continuously stratified laboratory ocean model,” *The Journal of the Acoustical Society of America* **141**(5), 3186–3189 (2017).
- <sup>13</sup> G. Rabau, “Scaled tank experiments of low-frequency propagation in the sofar channel,” *Acta Acustica united with Acustica* **85**(1), 12–17 (1999).
- <sup>14</sup> G. Real, X. Cristol, D. Habault, J.-P. Sessarego, and D. Fattaccioli, “Rafal: Random faced acoustic lens used to model internal waves effects on underwater acoustic propagation,” in *UACE2015 3rd Underwater Acoustics Conference & Exhibition* (2015).
- <sup>15</sup> G. Real, “An ultrasonic testbench for reproducing the degradation of sonar performance in a fluctuating ocean,” Ph.D. thesis, LMA CNRS UPR 7051, 2015.
- <sup>16</sup> J. Yangzhou, Z. Ma, and X. Huang, “A deep neural network approach to acoustic source localization in a shallow water tank experiment,” *The Journal of the Acoustical Society of America* **146**(6), 4802–4811 (2019).
- <sup>17</sup> C. T. Vongsawad, T. B. Neilsen, A. D. Kingsley, J. E. Ellsworth, B. E. Anderson, K. N. Terry, C. E. Dobbs, S. E. Hollingsworth, and G. H. Fronk, “Design of an underwater acoustics lab,” in *Proceedings of Meetings on Acoustics 181ASA*, Acoustical Society of America (2021), Vol. 45, p. 070005.
- <sup>18</sup> W. Marczak, “Water as a standard in the measurements of speed of sound in liquids,” *the Journal of the Acoustical Society of America* **102**(5), 2776–2779 (1997).
- <sup>19</sup> “Plastics - thermal conductivity coefficients” [https://www.engineeringtoolbox.com/thermal-conductivity-plastics-d\\_1786.html](https://www.engineeringtoolbox.com/thermal-conductivity-plastics-d_1786.html).
- <sup>20</sup> “Air - thermal conductivity vs. temperature and pressure” [https://www.engineeringtoolbox.com/air-properties-viscosity-conductivity-heat-capacity-d\\_1509.html](https://www.engineeringtoolbox.com/air-properties-viscosity-conductivity-heat-capacity-d_1509.html).
- <sup>21</sup> P. Ruiz Molina, J. Solé Rebull, P. Cervantes Fructuoso, and N. Ortega Ortega, “Method for the acoustic characterization of underwater sources in anechoic tanks based on simulated free-field scenario,” *Instrumentation Viewpoint* (18), 41–41 (2015).
- <sup>22</sup> G. Real, D. Habault, X. Cristol, J. Sessarego, and D. Fattaccioli, “An ultrasonic testbench for emulating the degradation of sonar performance in fluctuating media,” *Acta Acustica united with Acustica* **103**(1), 6–16 (2017).